JOURNAL OF NATURAL PRODUCTS

Article

pubs.acs.org/jnp

Halicloic Acids A and B Isolated from the Marine Sponge *Haliclona* sp. Collected in the Philippines Inhibit Indoleamine 2,3-Dioxygenase

David E. Williams,[†] Anne Steinø,[‡] Nicole J. de Voogd,[§] A. Grant Mauk,[‡] and Raymond J. Andersen*[,†]

[†]Departments of Chemistry and Earth, Ocean & Atmospheric Sciences, University of British Columbia, Vancouver, B.C., Canada, V6T 1Z1

[‡]Department of Biochemistry and Molecular Biology, University of British Columbia, Vancouver, B.C., Canada V6T 1Z3

[§]Netherlands Centre for Biodiversity Naturalis, P.O. Box 9517, 2300 RA, Leiden, The Netherlands

Supporting Information

ABSTRACT: Two new merohexaprenoids, halicloic acids A (**1**) and B (**2**), have been isolated from the marine sponge *Haliclona* (*Halichoclona*) sp. collected in the Philippines. The glycolic acids **1** and **2** slowly decomposed during acquisition of NMR data to aldehydes **3** and **4**, respectively, via an oxidative decarboxylation. Halicloic acid B (**2**) has the new rearranged "haliclane" meroterpenoid carbon skeleton. The halicloic acids **1** and **2** are indoleamine 2,3-dioxygenase inhibitors that are significantly more active than the decomposition products **3** and **4**.

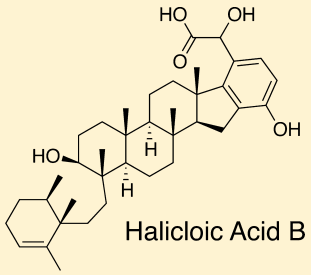

Immune escape plays an important role in cancer progression.[1,2] Tumor cells express many aberrant antigens that enable the immune system to recognize and remove them. However, the existence of benign or occult tumors, which can persist unchanged for many years, suggests there is an equilibrium between the tumor and the immune system whereby the tumor cannot completely escape the immune system and the immune system cannot completely remove the tumor. Immune surveillance generates a strong selective pressure for tumor cells that can evade immune destruction, and the genetic instability of tumor cells facilitates the acquisition of traits that eventually lead to immune escape. Once the tumors have escaped local and peripheral immune surveillance, invasion and metastasis can evolve, leading to progression of the cancer to a lethal outcome.

Mounting evidence indicates that indoleamine 2,3-dioxygenase (IDO) plays a central role in tumor-cell evasion of T cell-mediated immune rejection.[2,3] IDO catalyzes the oxidative cleavage of the 2,3 bond of tryptophan, which is the first and rate-limiting step in the kynurenine pathway of tryptophan catabolism in mammalian cells. T cell lymphocytes must divide to be activated. They are extremely sensitive to tryptophan shortage, which prevents their proliferation by causing them to undergo cell cycle arrest in G1. Localized IDO-mediated degradation of tryptophan at a tumor site is believed to inhibit T cell activation and proliferation and prevent immunological rejection of the tumor.

Expression of IDO is constitutively activated in a large number of human cancers.[2] IDO is also expressed by antigen-presenting cells at the periphery of tumors and in the lymph nodes that drain tumors, where appropriate T lymphocytes would otherwise be activated.[4] Marshalling the immune system against solid tumors is an attractive noncytotoxic approach to treating cancer, and therefore, inhibiting IDO has recently attracted much attention as a new strategy for anticancer drug development.[5,6] Data from murine cancer models have provided compelling in vivo proof of principle evidence for the promise of IDO inhibitors as anticancer drugs that used in combination with standard cytotoxic agents can enable the immune system to help regress established tumors.[3]

We have screened a library of extracts of marine invertebrates and laboratory cultures of microorganisms obtained from marine habitats with an in vitro assay for inhibition of human IDO as part of an ongoing program designed to discover new natural product IDO inhibitors. This screening program identified the annulins,[7] exiguamines,[8,9] and plectosphaeroic acids[10] as new classes of IDO inhibitors. Exiguamine A ($K_i \approx 40$ nM) remains one of the most potent IDO inhibitors known to date.

Extracts of the marine sponge *Haliclona* (*Halichoclona*) sp. (order Haplosclerida, family Chalinidae) collected in the Philippines also showed promising activity in the screening assay. Bioassay-guided fractionation of the extract identified halicloic acids A (**1**) and B (**2**) as IDO inhibitors. The halicloic acids **1** and **2** are new meroterpenoids that are related to the known compounds adociasulphates 2[11,12] and 10[13] and haliclotriol A.[14] Acids **1** and **2** cleanly decomposed to the aldehydes **3** and **4** during the acquisition of NMR data in DMSO-d_6. Details of the isolation, structure elucidation, chemical interconversions, and biological activities of the terpenoids **1**, **2**, **3**, and **4** are presented below.

RESULTS AND DISCUSSION

The sponge *Haliclona* (*Halichoclona*) sp. was harvested by hand using scuba on reefs off Culasian Point, Leyte, Philippines, and

Received: May 14, 2012
Published: August 7, 2012

frozen for transport and storage.[15] Lyophilized sponge tissue was exhaustively extracted with MeOH to give an extract that was active in the IDO inhibition assay. The dried residue from the MeOH extract was partitioned between H_2O and EtOAc. Fractionation of the IDO inhibitory EtOAc-soluble materials via Sephadex LH-20 chromatography followed by reversed-phase HPLC gave pure samples of halicloic acids A (**1**) and B (**2**).

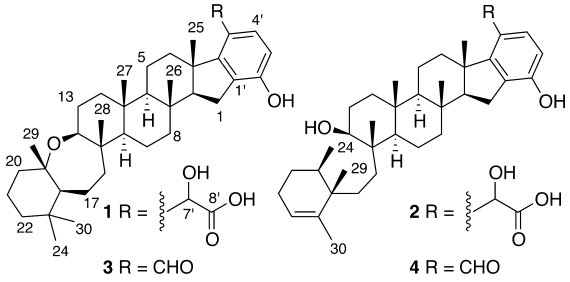

Halicloic acid A (**1**) was obtained as an optically active pale yellow glass that gave a $[M - H]^-$ ion in the HRESIMS at *m/z* 591.4054, appropriate for a molecular formula of $C_{38}H_{56}O_5$, requiring 11 sites of unsaturation. The initial ^1H NMR spectrum of **1**, recorded in DMSO-d_6 on material present in a single HPLC peak generated from a small-scale isolation, appeared as a 2:1 mixture of compounds **1** and **3**. After 24 h at room temperature (rt) in the NMR tube, the aldehyde **3** was the only compound that could be seen in the ^1H NMR spectrum of this sample.

Aldehyde **3** gave a $[M - H]^-$ peak at *m/z* 545.3990 in the HRESIMS, consistent with the molecular formula $C_{37}H_{54}O_3$, which differed from that of **1** by the loss of CH_2O_2 but still required 11 sites of unsaturation. The $^1H/^{13}C$/gCOSY/gHSQC/gHMBC NMR data obtained for **3** (Table 1) identified resonances that could be assigned to 37 carbon atoms, in agreement with the HRESIMS data. There were seven methyl singlets (δ 0.76, 0.81, 0.88, 0.93, 0.96, 1.05, 1.25) in the ^1H NMR spectrum of **3** recorded in C_6D_6. A downfield singlet at δ 10.41, which correlated to a carbon at δ 189.0 in the HSQC experiment, was assigned to a conjugated aldehyde. Vicinal methine doublets resonating at δ 7.89 and 6.43 (J = 8.3 Hz), which coupled to carbons at δ 130.1 and 113.8, respectively, in the HSQC, were assigned to a 3,4,5,6-tetrasubstituted aromatic ring. Oxygen-bearing quaternary (δ 77.4) and methine carbons (δ 3.43/73.7) were also apparent in the NMR data.

The ^1H NMR data for **3** acquired in DMSO-d_6 showed only a single proton resonance (δ 10.29, s, 2′-OH) that did not correlate to a carbon resonance in the gHSQC. This ^1H resonance was assigned to a phenol, and it showed gHMBC correlations to nonprotonated aromatic ring carbons resonating at δ 128.8 (C-1′), 158.9 (C-2′), and 113.5 (C-3′). Two of the three oxygen atoms in **3** were accounted for by the aldehyde and the phenol functionalities. The remaining oxygen atom had to be present as an ether linkage between the oxygenated aliphatic carbons. Five of the 11 sites of unsaturation in **3** were accounted for by the aldehyde and tetrasubstituted benzene ring. The lack of ^{13}C NMR evidence for other unsaturated functionalities required that **3** had to contain six additional rings.

Detailed analysis of the gCOSY and gHMBC NMR data obtained for aldehyde **3**, acquired in both C_6D_6 and DMSO-d_6, established the presence of a 4-hydroxy-2,3-disubstituted-benzaldehyde fragment, as shown in Figure 1. Subtracting the seven carbons assigned to this benzaldehyde residue from the 37 total carbons in the molecular formula showed that the remaining fragment of **3** had to contain 30 carbons and six additional rings. The presence of seven upfield methyl singlets in the ^1H NMR spectrum suggested that the 30-carbon fragment of **3** consisted of an oxygenated polycyclic hexaprenoid moiety.

In the gCOSY experiment, the benzylic H-1 proton signals were coupled to the H-2 methine resonance. The HMBC correlations from the methylene H-1 resonances to C-2 and C-3 (and C-7) and the two aromatic resonances assigned to C-1′ and C-6′ (and C-2′), together with the HMBC correlations from Me-25 to C-2, C-3, C-4, and the aromatic C-6′ resonance, defined the five-membered ring attached to the hydroxybenzaldehyde residue. The backbone of the hexaprenoid moiety and the positioning of four of the remaining five rings of the hexacyclic ring system were elucidated by piecing together the remaining four COSY-derived fragments by the series of gHMBC correlations shown in Figure 1. Finally, a gHMBC correlation between the carbon assigned to the quaternary carbon at C-19 and the resonance assigned to the H-14 methine established that the sixth and final ring was formed by an ether linkage between C-14 and C-19.

The relative configuration of aldehyde **3** was assigned from the tROESY correlations illustrated in Figure 2. Correlations were seen between the series of axial methyl groups from Me-25 to Me-28 as expected for an all-*trans-anti-trans* ring system. The large coupling constant observed in the H-14 multiplet (δ 3.43, dd, J = 11.9, 4.2 Hz) required H-14 to be axial. A strong tROESY correlation between H-14 and H-18 indicated that both protons were on the same α-face of the molecule. This along with the correlation between the two axial methyl signals, Me-24 and Me-29, completed the assignment of the relative configuration of aldehyde **3**.

We next turned our attention to the structure of halicloic acid A (**1**), the natural product precursor to aldehyde **3**. Halicloic acid A (**1**) was found to be stable in NMR solvents other than DMSO-d_6, but only poorly resolved NMR spectra that were not suitable for structural analysis were obtained in these solvents. In an attempt to circumvent the decomposition problem observed in DMSO-d_6, a portion of halicloic acid A (**1**) (2.1 mg) was dissolved in DMSO-d_6, and the collection of 1D and 2D NMR spectra was initiated immediately after the addition of the solvent. This approach generated a series of NMR spectra for **1** that indicated only ~5% of the parent compound had decomposed to **3** during the period of data acquisition. Over a period of several weeks in the NMR tube, this sample of **1** was completely converted to **3**.

In the NMR spectra of **1**, the resonances assigned to the aldehyde moiety in **3** were replaced by a series of additional signals. These included a proton resonance at δ 5.21 (H-7′), which was coupled to an exchangeable proton resonance at δ 5.38 in the gCOSY experiment, correlated to a carbinol methine (C-7′: δ 67.7) in the gHSQC, and correlated to a carbon resonance at δ 175.0 (C-8′) in the gHMBC experiment. Replacement of the aldehyde group in **3** with a glycolic acid residue in **1** satisfied the differences in both the NMR analysis and the (−)-HRESIMS difference of CH_2O_2 between the two compounds. Additional HMBC correlations from H-7′ (δ 5.21) to the aromatic resonances assigned to C-4′ (δ 126.3), C-5′ (δ 125.6), and C-6′ (δ 153.1) and between H-4′ (δ 6.86) and C-7′ (δ 67.7) confirmed the location of the glycolic acid side chain at C-5′. All attempts to

dx.doi.org/10.1021/np300345j | J. Nat. Prod. 2012, 75, 1451−1458

Table 1. ^{1}H (600 MHz) and ^{13}C (150 MHz) NMR Data for Halicloic Acid A (1) and Aldehyde 3

	1		3			
	DMSO-d_6		DMSO-d_6		C_6D_6	
position	δ_C	δ_H (J in Hz)	δ_C	δ_H (J in Hz)	δ_C	δ_H (J in Hz)
1α	24.2	2.47, dd (13.4, 6.0)	24.3	2.53, dd (14.0, 5.8)	24.6	2.61, dd (14.3, 6.2)
1β		2.32, dd (13.4, 13.4)		2.41, dd (14.0, 14.0)		2.37, dd (14.3, 14.3)
2	63.5	1.55, nd[a]	63.6	1.61, nd	64.1	1.58, nd
3	48.0		48.7		49.3	
4_{ax}	38.6	1.75, td (11.8, 3.2)	38.9	1.65, nd	39.7	1.59, nd
4_{eq}		2.29, nd		2.53, nd		2.41, bd (12.3)
5	18.2	1.55−1.60	18.2	1.60, nd	18.9	1.34, nd
		1.55−1.60		1.60, nd		1.44, nd
6	60.4	0.84, nd	60.3	0.86, nd	60.9	0.64, bd (13.3)
7	36.7		36.7		37.3	
8_{ax}	41.5	1.04, nd	41.4	1.05, nd	42.2	0.88, nd
8_{eq}		1.57, nd		1.59, nd		1.53, nd
9	17.4	1.44−1.50	17.4	1.46−1.52	18.1	1.37, nd
		1.44−1.50		1.46−1.52		1.45, nd
10	56.8	0.79, bd (13.2)	56.8	0.79, dd (12.3, 2.1)	57.7	0.62, bd (12.6)
11	36.6		36.5		37.2	
12_{ax}	38.3	0.94, nd	38.3	0.93, nd	39.0	0.79, nd
12_{eq}		1.60, nd		1.60, nd		1.57, nd
13_{ax}	27.1	1.53, nd	27.0	1.55, nd	27.8	1.86, qm (11.9)
13_{eq}		1.25, nd		1.26, nd		1.56, nd
14	72.7	3.47, dd (11.2, 4.3)	72.7	3.47, dd (11.2, 4.3)	73.7	3.43, dd (11.9, 4.2)
15	41.1		41.1		41.9	
16_{ax}	44.6	0.76, nd	44.6	0.75, nd	45.8	0.77, nd
16_{eq}		1.66, bd (13.0)		1.66, bd (13.0)		1.72, bdd (12.6, 2.7)
17_{ax}	19.4	1.35, nd	19.4	1.34, nd	20.3	1.53, nd
17_{eq}		1.35, nd		1.34, nd		1.36, nd
18	52.9	1.43, nd	52.9	1.43, nd	54.3	1.41, nd
19	76.7		76.7		77.4	
20_{ax}	37.8	1.35, nd	37.7	1.35, nd	38.7	1.63, bd (12.1)
20_{eq}		1.35, nd		1.35, nd		1.40, nd
21_{ax}	20.8	1.44−1.50	20.8	1.47−1.49	21.7	1.48, nd
21_{eq}		1.44−1.50		1.47−1.49		1.43, nd
22_{ax}	40.4	1.10, td (13.0, 4.4)	40.4	1.10, td (13.1, 4.8)	41.4	1.06, nd
22_{eq}		1.27, nd		1.27, nd		1.26, nd
23	35.2		35.2		35.7	
24	21.0	0.73, s	20.9	0.73, s	21.2	0.76, s
25	21.6	1.05, s	22.0	1.13, s	22.3	1.05, s
26	16.9	0.98, s	16.9	1.01, s	17.3	0.88, s
27	16.1	0.83, s	16.0	0.83, s	16.4	0.81, s
28	14.5	0.71, s	14.4	0.71, s	14.9	0.96, s
29	23.0	1.03, s	23.0	1.03, s	23.5	1.25, s
30	32.7	0.89, s	32.7	0.89, s	33.2	0.93, s
1′	127.4		128.8		129.0	
2′	153.0		158.9		157.8	
3′	112.7	6.50, d (8.5)	113.5	6.70, d (8.5)	113.8	6.43, d (8.3)
4′	126.3	6.86, d (8.5)	129.3	7.51, d (8.5)	130.1	7.89, d (8.3)
5′	125.6		124.0		126.3	
6′	153.1		159.3		159.9	
7′	67.7	5.21, bs	189.4	10.12, s	189.0	10.41, s
8′	175.0					
2′-OH		9.08, s		10.29, s		5.86, bs
7′-OH		5.38, bs				
8′-COOH		12.26, bs				

[a]Multiplicity not determined due to overlapping signals/chemical shifts determined from 2D data.

determine the absolute configuration at C-7′ of halicloic acid A (1) by forming Mosher's esters at the 7′-hydroxy group were unsuccessful.

The HRESIMS spectrum of halicloic acid B (2) gave a $[M - H]^-$ ion at m/z 591.4039, consistent with the molecular formula $C_{38}H_{56}O_5$, which was the same molecular formula found for

dx.doi.org/10.1021/np300345j | J. Nat. Prod. 2012, 75, 1451−1458

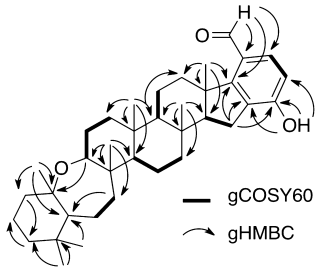

Figure 1. Selected 2D NMR correlations observed for aldehyde **3**.

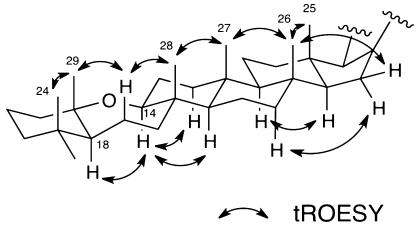

Figure 2. Selected tROESY correlations observed for aldehyde **3**.

halicloic acid A (**1**). Over a period of weeks, halicloic acid B (**2**) dissolved in DMSO-d_6 decomposed to the aldehyde **4**, mimicking the behavior of halicloic acid A (**1**). Detailed analysis of the 1D and 2D NMR spectra obtained for **2** (Table 2) showed that **1** and **2** were identical in all parts except for the A and B rings.

An olefinic methyl resonance at δ 1.58 (Me-30) in the ^{1}H NMR spectrum of **2** showed gHMBC correlations to resonances assigned to C-18 (δ 39.6), C-19 (δ 139.9), and C-20 (δ 123.0), and a gCOSY correlation to an olefinic methine resonance at δ 5.30 (H-20). H-20 (δ 5.30) was in turn correlated in the gCOSY spectrum to the allylic methylene resonances assigned to H-21 (δ 1.85/1.91) and in the gHMBC spectrum to resonances assigned to C-21 (δ 25.1), C-22 (δ 26.7), and C-18 (δ 39.6). A pair of singlets assigned to the *gem*-dimethyl group in the ^{1}H NMR spectrum of **1** were replaced by a methyl doublet [Me-24: δ 0.78 (J = 6.7 Hz)] and a methyl singlet (Me-29: δ 0.78) in the ^{1}H NMR spectrum of **2**. The doublet (δ 0.78), assigned to Me-24 in **2**, correlated in the gHMBC experiment to carbon resonances assigned to C-22 (δ 26.7), C-23 (δ 32.7), and C-18 (δ 39.6). gHMBC correlations were observed between the singlet (δ 0.78), assigned to Me-29, and carbon resonances assigned to C-18 (δ 39.6), C-19 (δ 139.9), C-23 (δ 32.7), and C-17 (δ 28.2). The C-17 resonance was coupled to proton resonances at δ 1.07/1.28 in the gHSQC experiment. Taken together, the 2D correlations described above led to the conclusion that the A ring in **2** was a 2,3,4-trimethyl-4-alkylcyclohexene fragment.

The ^{1}H NMR data of halicloic acid B (**2**) contained a second proton resonance (δ 4.06, d, J = 4.9) that was not correlated to a carbon resonance in the gHSQC spectrum. This resonance,

Table 2. ^{1}H (600 MHz) and ^{13}C (150 MHz) NMR Data for Halicloic Acid B (2) and Aldehyde 4

	2[a]		**4**[b]	
position	δ_C	δ_H (J in Hz)	δ_C	δ_H (J in Hz)
1α	24.2	2.39, nd[c]	24.3	2.38, dd (13.1, 6.2)
1β		2.32, dd (13.7, 13.7) 1313.7)		2.24, dd (13.1, 13.1)
2	63.6	1.57, nd	63.3	1.24, dd (13.1, 6.2)
3	48.0		49.2	
4_{ax}	38.6	1.79, nd	39.3	1.49, nd
4_{eq}		2.29, bd (12.5)		2.35, bd (12.1)
5	18.3	1.53−1.57	18.8	1.32, nd
		1.53−1.57		1.36, nd
6	60.7	0.90, nd	60.8	0.53, bd (11.9)
7	36.8		37.3	
8	41.1	1.07, nd	41.4	0.91, nd
		1.59, nd		1.47, nd
9	17.1	1.30, nd	17.7	1.36, nd
		1.46, nd		1.36, nd
10	49.4	0.93, nd	50.1	0.86, dd (11.5, 7.4)
11	36.5		37.0	
12_{ax}	37.7	0.88, nd	38.4	0.69, m
12_{eq}		1.58, nd		1.48, nd
13	27.2	1.50, nd	27.9	1.44, nd
		1.50, nd		1.44, nd
14	71.0	3.26, nd	72.5	3.42, dd (9.3, 6.4)
15	40.2		41.1	
16	30.0	1.03, nd	30.8	1.32, nd
		1.17, nd		1.51, nd
17	28.2	1.07, nd	29.1	1.30, nd
		1.28, nd		1.51, nd
18	39.6		40.6	
19	139.9		140.0	
20	123.0	5.30, bs	124.4	5.52, bs
21	25.1	1.85, m	26.1	1.95, m
		1.91, m		2.04, m
22	26.7	1.37, nd	27.6	1.44, nd
		1.37, nd		1.49, nd
23	32.7	1.71, m	33.6	1.91, m
24	15.8	0.78, d (6.7)	16.3	0.96, d (6.8)
25	21.6	1.05, s	22.2	1.03, s
26	16.9	0.98, s	17.2	0.83, s
27	16.5	0.83, s	16.7	0.74, s
28	17.6	0.66, s	17.6	0.78, s
29	21.2	0.78, s	21.8	1.03, s
30	18.8	1.58, bs	19.3	1.85, bs
1′	127.4		128.9	
2′	152.9		157.7	
3′	112.8	6.50, d (8.5)	113.7	6.48, d (8.4)
4′	126.3	6.86, d (8.5)	130.1	7.89, d (8.4)
5′	125.6		126.3	
6′	153.1		159.9	
7′	67.6	5.21, d (4.6)	189.0	10.39, s
8′	175.0			
14-O<u>H</u>		4.06, d (4.9)		
2′-O<u>H</u>		9.04, s		5.74, bs
7′-O<u>H</u>		5.38, d (4.6)		
8′-COO<u>H</u>		12.29, bs		

[a]Spectra collected in DMSO-d_6. [b]Spectra collected in C_6D_6. [c]Multiplicity not determined due to overlapping signals/chemical shifts determined from 2D data.

dx.doi.org/10.1021/np300345j | *J. Nat. Prod.* 2012, 75, 1451−1458

assigned to the OH of a secondary alcohol, showed correlations to carbinol methine resonances at δ 3.26 (H-14) and 71.0 (C-14) in the gCOSY and gHMBC experiments, respectively. The ^{1}H resonance assigned to Me-28 (δ 0.66) showed gHMBC correlations as expected to the C-14 carbinol methine (δ 71.0) and to the C-10 (δ 49.4), C-15 (δ 40.2), and C-16 (δ 30.0) resonances. gHSQC correlations were observed between the C-16 resonance (δ 30.0) and the H-16 proton resonances at δ 1.03/1.17. gCOSY correlations observed between the H-16 protons (δ 1.03/1.17) and the H-17 methylene protons (δ 1.07/1.28) of the C-4 alkyl substituent of the cyclohexene A ring established that a bridge of two methylene groups linked the A and C rings between C-15 and C-18, completing the constitution of **2**. The decomposition product of halicloic acid B (**2**) was assigned the structure **4** by analogy with the established decomposition of halicloic acid A (**1**) to aldehyde **3**.

Comparison of the NMR assignments for **1** and **2** (Tables 1 and 2) and analysis of the 2D ROESY data recorded for **2** established that the relative configurations across rings C to F in **2** and **4** were the same as in **1** and **3**, as shown. The relative configuration of the A ring cyclohexene methyls was deduced by comparison of the ^{13}C NMR chemical shifts for **2** with those of other natural products containing a similarly substituted cyclohexene ring. Figure 3 illustrates that on the basis of this

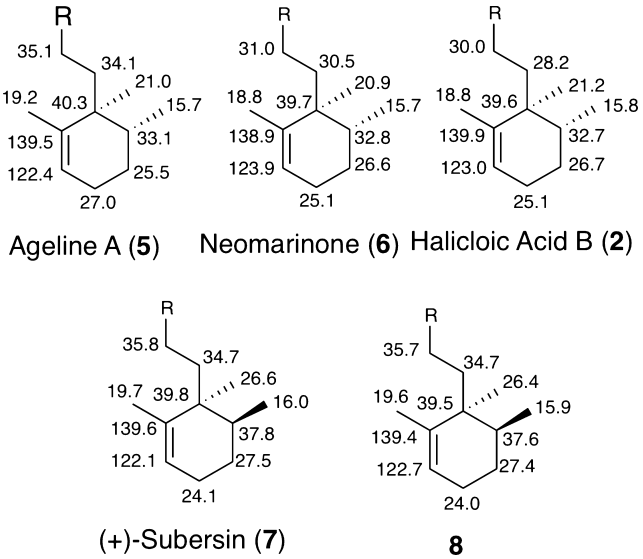

Figure 3. Comparison of ^{13}C NMR chemical shifts of the 1,2,5-trimethyl-6-alkylcyclohex-1,2-ene fragment of halicloic acid B (**2**) with model compounds.

comparison the *cis* relative configuration for the two aliphatic methyls reported for the sponge metabolite ageline A[16] (**5**) and the filamentous bacterial metabolite neomarinone (**6**)[17,18] is favored in **2** over the *trans* relationship reported for the sponge metabolites (+)-subersin (**7**)[19] and **8**.[20]

Although a strong ROESY correlation was observed between the vinylic Me-30 on ring A and the axially orientated H-14 (dd, J = 9.3, 6.4 Hz) of the C ring carbinol, it was not possible to unambiguously relate the relative configuration of ring A to that of C. Attempts at forming Mosher's esters at the C-14 and/or C-7′-hydroxy in **2** were unsuccessful. Scheme 1 shows a proposed biogenesis for the halicloic acids. If one assumes that the same carbocation intermediate **III** leads to **1** and **2** and that the Wagner−Meerwien 1,2 proton and methyl

Scheme 1. Proposed Late-Stage Biogenesis for Halicloic Acids A (1) and B (2)

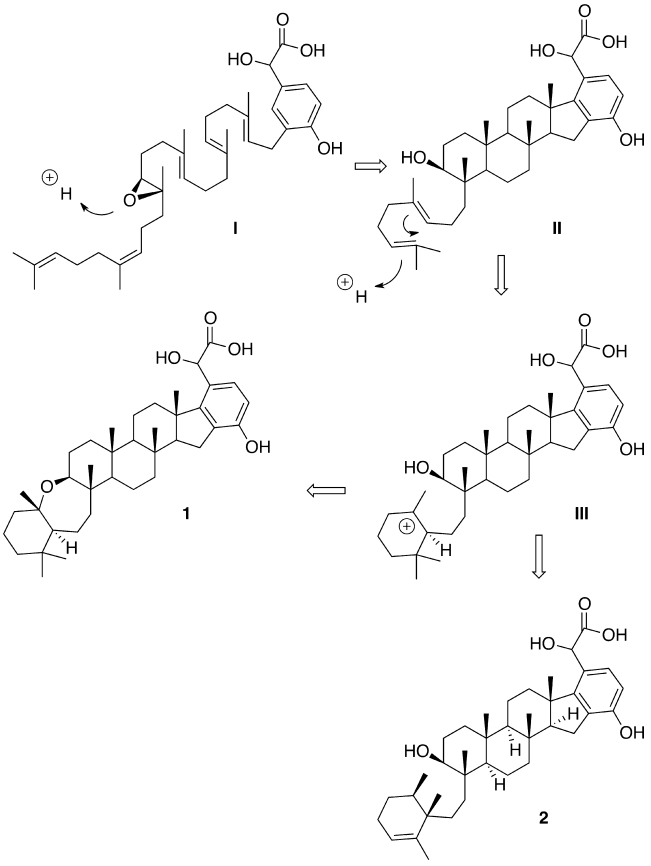

migrations required to convert **III** to **2** are both suprafacial, then this biogenetic proposal suggests that the complete relative configuration of halicloic acid B (**2**) can be assigned as 2*S**,3*S**,6*S**,7*R**,10*R**,11*S**,14*S**15*S**,18*S**,23*R**, as shown.

The oxidative decarboxylation of vanillylmandelic acid (3-methoxy-4-hydroxymandelic acid) to vanillin (3-methoxy-4-hydroxybenzaldehyde) in the presence of sodium metaperiodate is a well-known industrial process. Two mechanisms have been proposed for this conversion. In both cases, the oxidative decarboxylation would proceed through a concerted mechanism after the formation of a reaction intermediate in which the hypervalent iodine atom is covalently attached to the phenoxide oxygen or to two of the oxygen atoms of the glycolic acid residue. Current evidence favors the former in neutral or alkaline media, as the presence of the phenol functionality is crucial.[21,22] As described above, halicloic acids A (**1**) and B (**2**) undergo complete conversion to aldehydes **3** and **4**, respectively, when left standing in DMSO-d_6 in the presence of trace amounts of TFA (remaining after evaporation of HPLC solvents) at 4 °C or at rt. No reaction was observed when mandelic acid or 4-hydroxymandelic acid was reacted under these same mild conditions with or without TFA. However, when a DMSO solution of 4-hydroxymandelic acid containing trace amounts of TFA was heated, a 5% yield of 4-hydroxybenzaldehyde was obtained.

Scheme 2 shows a proposed mechanism for the oxidative decarboxylation of **1** and **2** that involves the trifluoracetyldimethylsulfoxide intermediate **10** in the Moffat−Swern oxidation. This proposal suggests that TFA can react with the phenol

dx.doi.org/10.1021/np300345j | *J. Nat. Prod.* 2012, 75, 1451−1458

Scheme 2. Proposed Mechanism for the Oxidative Decarboxylation of Halicloic Acids A (1) and B (2) in the Presence of DMSO/TFA

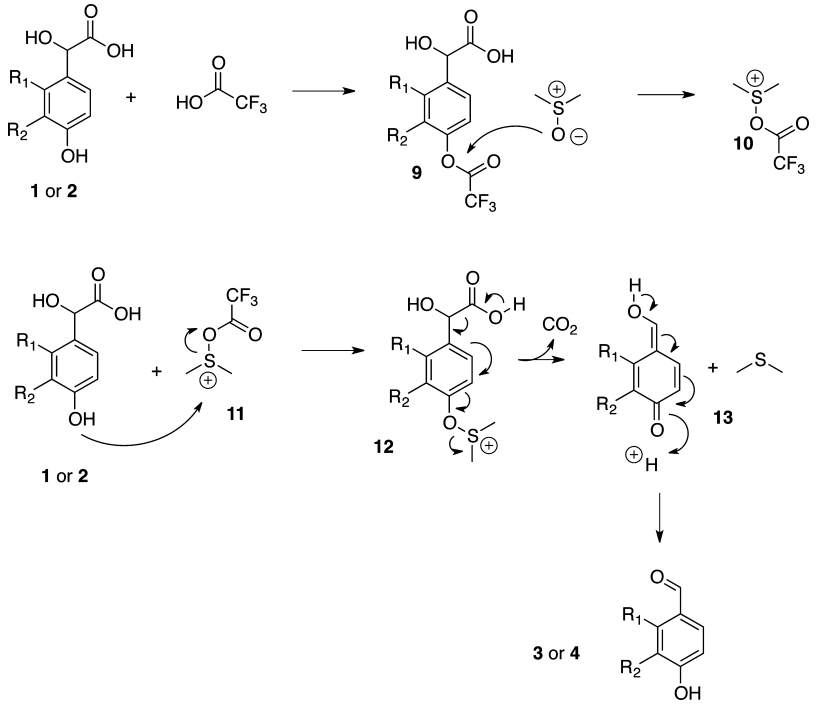

in **1** or **2** to give TFA ester **9**, which can then react with DMSO to give the Moffat−Swern intermediate **10**. Literature reports and our own observations indicate that the *para*-phenol functionality is required for the oxidative decarboxylation of mandelic acid under the DMSO/TFA conditions. Therefore, we have assumed that the intermediate sulfonium ion **10** reacts with the phenol functionality in **1** and **2** to give sulfonium ion intermediates **12**. Decarboxylation of intermediates **12** with simultaneous loss of dimethyl sulfide can generate the *p*-quinomethides **13**, which after tautomerization gives the aldehyde decomposition products **3** and **4**.

Halicloic acids A (**1**) and B (**2**), aldehydes **3** and **4**, mandelic acid, 4-hydroxymandelic acid, benzaldehyde, and 4-hydroxybenzaldehyde were all assayed for in vitro inhibition of purified recombinant human IDO (Figure 4). Halicloic acids A (**1**) and B (**2**) had IC_{50}'s of 10 and 11 μM, respectively, in the assay. Aldehydes **3** and **4** were significantly less active, with IC_{50}'s of 53 and 29 μM, respectively, while mandelic acid, 4-hydroxymandelic acid, benzaldehyde, and 4-hydroxybenzaldehyde were all inactive at the highest concentration tested (200 μM), indicating that the hexaprenoid moiety in **1** and **2** is critical for IDO inhibition.

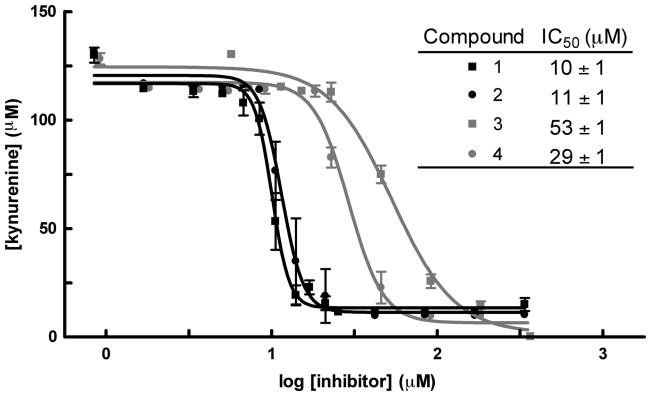

Figure 4. In vitro inhibition of IDO activity by compounds **1**, **2**, **3**, and **4**. Nonlinear regression curves were based on a sigmoidal dose−response equation and used to calculate the corresponding IC_{50} values of compounds **1**−**4**, shown in the table. The data are shown as an average of quadruplicates with error bars representing SD.

Halicloic acids A (**1**) and B (**2**) are new meroterpenoids composed of 4-hydroxymandelic acid and cyclized hexaprenoid components. Halicloic acid A (**1**) has the same meroterpenoid carbon skeleton as adociasulfate-7, and its hexaprenoid fragment is identical to that found in adociasulfate-2.[11−13] Halicloic acid B (**2**) has the new rearranged "haliclane" meroterpenoid carbon skeleton. Halicloic acids A (**1**) and B (**2**) are low μM in vitro inhibitors of IDO, and they represent a new natural product template that can be used to guide the design of synthetic inhibitors of IDO.

EXPERIMENTAL SECTION

General Experimental Procedures. Optical rotations were measured using a Jasco P-1010 polarimeter with sodium light (589 nm). UV spectra were recorded with a Waters 996 photodiode array detector. The ^{1}H and ^{13}C NMR spectra were recorded on a Bruker AV-600 spectrometer with a 5 mm CPTCI cryoprobe. ^{1}H chemical shifts are referenced to the residual C_6D_6 or DMSO-d_6 signal (δ 7.15 and 2.49 ppm, respectively), and ^{13}C chemical shifts are referenced to the C_6D_6 or DMSO-d_6 solvent peak (δ 128.0 or 39.5 ppm, respectively). Low- and high-resolution ESI-QIT-MS were recorded on a Bruker-Hewlett-Packard 1100 Esquire-LC system mass spectrometer. Merck type 5554 silica gel plates and Whatman MKC18F plates were used for analytical thin layer chromatography. Reversed-phase HPLC purifications were performed on a Waters 600E System Controller liquid chromatograph attached to a Waters 996 photodiode array detector using a flow rate of 2.0 mL/min. All solvents used for HPLC were Fisher HPLC grade and were filtered through a 0.45 μm filter (Osmonics Inc.) prior to use.

Sponge Material. The sponge was collected by hand using scuba near Culasian Point, Leyte, Philippines, in March 1991 (S 11°19.00′,

dx.doi.org/10.1021/np300345j | J. Nat. Prod. 2012, 75, 1451−1458

E 124°35.60′). The lavender-colored sponge is thickly encrusting across a coral fragment. Consistency is firm and crisp and breaks easily. The sponge was identified as *Haliclona* (*Halichoclona*) sp. POR6118 (family Chalinidae, order Haplosclerida). The ectosomal skeleton is a tangential subisotropic reticulation of single spicules cemented at the nodes with spongin. The choanosome consists of a subisotropic paucispicular skeleton with ill-defined primary and secondary lines with many loose spicules in confusion. The spicules are stout oxeas that are abruptly pointed with a dimension of 190−210 × 8−10 μm. At least 53 species belonging to the genus of *Haliclona* have been reported in the Philippines and neighboring areas (Central Indo Pacific), and only two belong to the same subgenus *Halichoclona*. *Haliclona* (*Halichoclona*) *vanderlandi* de Weerdt & van Soest, 2002 from Indonesia has similar spicule dimensions (175−218 × 6−10 μm), but its growth form is tubular. *Haliclona* (*Halichoclona*) *centragulata* (Sollas, 1902) from Malaysia also has similar spicule dimensions, 220 × 7 μm, but has sigmoid microscleres in addition. Eight species hve been reported from the Philippines, and none of these fit the present species. In conclusion, the present sponge might very well be an undescribed species. A voucher sample has been deposited at The Netherlands Centre for Biodiversity Naturalis in Leiden, The Netherlands (voucher number: RMNH POR. 6118).

Small-Scale Extraction of the Sponge and Isolation of Halicloic Acids A (1) and B (2). Freshly collected sponge was frozen on site and transported frozen. Lyophilized sponge material (10 g) was cut into small pieces and immersed in and subsequently extracted repeatedly with MeOH (3 × 50 mL) at rt. The combined MeOH extracts were concentrated *in vacuo*, and the resultant residue was then partitioned between EtOAc (3 × 5 mL) and H_2O (15 mL). The combined EtOAc extract was evaporated to dryness, and the resulting oil was chromatographed on Sephadex LH-20 with 4:1 MeOH/CH_2Cl_2 as eluent. Purification of the active fraction via C_8 reversed-phase HPLC using a Phenomenex 5 μm, Luna 25 × 1.0 cm column, with 3:1 MeCN/(0.05%TFA/H_2O) as eluent, gave pure samples of halicloic acids A (**1**) (0.5 mg) and B (**2**). However, the yield of B provided us with only enough material to obtain a very weak ^{1}H NMR spectrum.

Decomposition of Halicloic Acid A (1) to Aldehyde 3. After lyophilizing halicloic acid A (**1**) overnight in an NMR tube and adding 600 μL of DMSO-d_6, **1** was observed to decompose cleanly to aldehyde **3** within 24 h at 4 °C.

Larger Scale Extraction of the Sponge and Isolation of Halicloic Acids A (1) and B (2). The larger scale workup started with 32 g of lyophilized sponge material and proceeded as described above to yield 15.8 and 3.7 mg of halicloic acids A (**1**) and B (**2**), respectively.

Controlled Decomposition of Halicloic Acids A (1) and B (2) to Aldehydes 3 and 4, Respectively. Halicloic acids A (**1**) and B (**2**) appeared stable when the two samples were dried down directly in NMR tubes and spectra acquired in MeOH-d_4 or in mixtures of MeOH-d_4/CD_2Cl_2. The spectra obtained in these NMR solvents were, however, poorly resolved, with broad peaks and of no use for structural elucidation. With this in mind, after both **1** and **2** had first been dried overnight in separate NMR tubes on a freeze drier, 600 μL of DMSO-d_6 was added to an additional 2.1 mg of halicloic acid A (**1**) and to 0.6 mg of halicloic acid B (**2**). Immediately after the addition of the DMSO-d_6, 1D and 2D NMR spectra were run for both samples. Fortunately, this time, for both samples there was only partial conversion after 16 h of collecting NMR data (5% and 20%, for **1** and **2**, respectively). Then over a period of several weeks initially at 4 °C and later at rt both **1** and **2** were observed to cleanly convert to aldehydes **3** and **4**, respectively.

Halicloic acid A (1): pale yellow glass; $[\alpha]^{25}_D$ −66 (*c* 6.1, MeOH); UV (3:1 MeCN/(0.05%TFA/H_2O)) λ_{max} 208, 224, 272 nm; ^{1}H and ^{13}C NMR, see Table 1; (−)-HRESIMS *m*/*z* 591.4054 $[M - H]^-$ (calcd for $C_{38}H_{55}O_5$, 591.4050).

Halicloic acid B (2): pale yellow glass; $[\alpha]^{25}_D$ −5.0 (*c* 2.1, MeOH); UV (3:1 MeCN/(0.05%TFA/H_2O)) λ_{max} 208, 224, 272 nm; ^{1}H and ^{13}C NMR, see Table 2; (−)-HRESIMS *m*/*z* 591.4039 $[M - H]^-$ (calcd for $C_{38}H_{55}O_5$, 591.4050).

Aldehyde 3: pale yellow glass; $[\alpha]^{25}_D$ −51 (*c* 1.1, 3:1 CH_2Cl_2/MeOH); ^{1}H and ^{13}C NMR, see Table 1; (−)-HRESIMS *m*/*z* 545.3990 $[M - H]^-$ (calcd for $C_{37}H_{53}O_3$, 545.3995).

Aldehyde 4: pale yellow glass; $[\alpha]^{25}_D$ +42 (*c* 0.3, 3:1 CH_2Cl_2/MeOH); ^{1}H and ^{13}C NMR, see Table 2; (−)-HRESIMS *m*/*z* 545.3989 $[M - H]^-$ (calcd for $C_{37}H_{53}O_3$, 545.3995).

Treatment of Both Mandelic Acid and 4-Hydroxymandelic Acid with DMSO-d_6, with and without Trace Amounts of TFA. To dried 10 mg samples of D/L-mandelic acid and 4-hydroxymandelic acid was added 600 μL of 4:1 MeCN/(0.05%TFA/H_2O), and the samples were immediately dried. Similarly, to dried 10 mg samples of D/L-mandelic acid and 4-hydroxymandelic acid was added 600 μL of 4:1 MeCN/H_2O, and again the samples were immediately dried. To each of the four dried samples was added 600 μL of DMSO-d_6, and the samples were left to sit at rt for 7 days. Each sample was then heated to 50 °C for 7 days, followed by 78 °C for 4 days, and finally 128 °C for 4 days. The resulting reaction mixture obtained for the sample of 4-hydroxymandelic acid treated with 4:1 MeCN/(0.05% TFA/H_2O) was the only sample to show both appreciable decomposition and the significant production of an aromatic aldehyde as determined by the observation of a singlet resonating at δ 9.76 ppm and the concomitant appearance of an aromatic doublet at δ 7.74 ppm in the ^{1}H NMR spectrum. These diagnostic resonances, though only small, were initially seen after heating to 50 °C for 7 days and increased in size as the temperature increased. The experiments were terminated when there appeared to be enough of the desired product to isolate. The sample was purified using Si gel flash chromatography (step gradient 19:1 hexanes/EtOAC to EtOAc to 1:9 MeOH/EtOAc, 2 g Sep pak). An early eluting fraction (19:1−9:1 hexanes/EtOAc) was further purified via C_8 reversed-phase HPLC, using a CSC-Inertsil 150A/ODS2 5 μm 25 × 0.94 cm column, with 17:3 H_2O/MeCN as eluent to give 4-hydroxybenzaldehyde (0.5 mg), which was identified by co-injection and comparison with the UV and NMR spectra of a standard sample.

IDO Inhibition Assays. Enzyme activity assays were performed with human recombinant IDO (rh-IDO) expressed in *E. coli* as previously described.[23] The activity of rh-IDO in the absence and presence of inhibitory compounds was determined using an end-point assay as previously described[24] with the following changes: The assay was performed in 100 mM potassium phosphate buffer (pH 6.5) containing 10 mM sodium ascorbate (Sigma), 1.25 μM methylene blue (Sigma), 10 μg/mL catalase (Sigma), and 400 μM L-tryptophan (Sigma). The reaction was started by the addition of rh-IDO (100 nM) and allowed to progress at 37 °C for 60 min before termination with 30% (w/v) trichloroacetic acid. The samples were further incubated for 15 min at 60 °C prior to addition of 2% (w/v) 4-(dimethylamino)-benzaldehyde (Sigma). After 5 min at rt, the absorbance at 480 nm was measured with a Tecan infinite M200 plate reader, and the kynurenine concentration was determined from the extinction coefficient (15 820 M^{-1} cm^{-1}) for kynurenine.[25] Nonlinear regression of the enzyme activity assays and calculations of IC_{50} values were performed using GraphPad Prism 4.

■ ASSOCIATED CONTENT

Ⓢ Supporting Information

^{1}H, ^{13}C, and 2D NMR spectra of compounds **1**, **2**, **3**, and **4**. This material is available free of charge via the Internet at http://pubs.acs.org.

■ AUTHOR INFORMATION

Corresponding Author

*Tel: 604 822 4511. Fax: 604 822 6091. E-mail: raymond.andersen@ubc.ca.

Notes

The authors declare no competing financial interest.

■ ACKNOWLEDGMENTS

Financial support was provided by Canadian Cancer Research Institute grants to R.J.A. and A.G.M. R.J.A. thanks Pfizer for the generous gift of marine invertebrate specimens.

■ REFERENCES

(1) Prendergast, G. C. *Oncogene* **2008**, *27*, 3889−3900.
(2) Uyttenhove, C.; Pilotte, L.; Theate, I.; Stroobant, V.; Colau, D.; Parmentier, N.; Boon, T.; van den Eynde, B. *Nat. Med.* **2003**, *9*, 1269−1274.
(3) Muller, A. J.; DuHadaway, J. B.; Donover, P. S.; Sutanto-Ward, E.; Prendergast, G. C. *Nat. Med.* **2005**, *11*, 312−319.
(4) Munn, D. H.; Sharma, M. D.; Hou, D.; Baban, B.; Lee, J. R.; Antonia, S. J.; Messina, J. L.; Chandler, P.; Koni, P. A.; Mellor, A. L. *J. Clin. Invest.* **2004**, *114*, 280−290.
(5) Muller, A. J.; Prendergast, G. C. *Cancer Res.* **2005**, *65*, 8065−8068.
(6) Muller, A. J.; Malachowski, W. P.; Prendergast, G. C. *Expert Opin. Ther. Targets* **2005**, *9*, 831−849.
(7) Pereira, A.; Vottero, E.; Roberge, M.; Mauk, A. G.; Andersen, R. J. *J. Nat. Prod.* **2006**, *69*, 1496−1499.
(8) Brastianos, H. C.; Vottero, E.; Patrick, B. O.; Van Soest, R.; Matainaho, T.; Mauk, A. G.; Andersen, R. J. *J. Am. Chem. Soc.* **2006**, *128*, 16046−16047.
(9) Volgraf, M.; Lumb, J.-P.; Brastianos, H. C.; Carr, G.; Chung, M. K. W.; Münzel, M.; Mauk, A. G.; Andersen, R. J.; Trauner, D. *Nat. Chem. Biol.* **2008**, *4*, 535−537.
(10) Carr, G.; Tay, W.; Bottriell, H.; Andersen, S. K.; Mauk, A. G.; Andersen, R. J. *Org. Lett.* **2009**, *11*, 2996−2999.
(11) Sakowicz, R.; Berdelis, M. S.; Ray, K.; Blackburn, C. L.; Hopmann, C.; Faulkner, D. J.; Goldstein, L. S. B. *Science* **1998**, *280*, 292−295.
(12) Blackburn, C. L.; Hopmann, C.; Sakowicz, R.; Berdelis, M. S.; Goldstein, L. S. B.; Faulkner, D. J. *J. Org. Chem.* **1999**, *64*, 5565−5570.
(13) Blackburn, C. L.; Faulkner, D. J. *Tetrahedron* **2000**, *56*, 8429−8432.
(14) Crews, P.; Harrison, B. *Tetrahedron* **2000**, *56*, 9039−9046.
(15) The sponge specimens were collected under contracts with the Pfizer research laboratories in St. Louis. When Pfizer disbanded its natural products program, they generously donated their marine invertebrate collection to Andersen's group at UBC.
(16) Capon, R. J.; Faulkner, D. J. *J. Am. Chem. Soc.* **1984**, *106*, 1819−1822.
(17) Kalaitzis, J. A.; Hamano, Y.; Nilsen, G.; Moore, B. S. *Org. Lett.* **2003**, *5*, 4449−4452.
(18) Hardt, I. H.; Jensen, P. R.; Fenical, W. *Tetrahedron Lett.* **2000**, *41*, 2073−2076.
(19) Caroll, J.; Jonsson, E. N.; Ebel, R.; Hartman, M. S.; Holman, T. R.; Crews, P. *J. Org. Chem.* **2001**, *66*, 6847−6851.
(20) Carotenuto, A.; Conte, M. R.; Fattorusso, E.; Lanzotti, V.; Magno, S. *Tetrahedron* **1995**, *51*, 10751−10758.
(21) Taran, F.; Renard, P. Y.; Bernard, H.; Mioskowski, C.; Frobert, Y.; Pradelles, P.; Grassi, J. *J. Am. Chem. Soc.* **1998**, *120*, 3332−3339.
(22) Favier, I.; Giulieri, F.; Duñach, E.; Hébroult, D.; Desmurs, J.-R. *Eur. J. Org. Chem.* **2002**, 1984−1988.
(23) Vottero, E.; Balgi, A.; Woods, K.; Tugendreich, S.; Melese, T.; Andersen, R. J.; Mauk, A. G.; Roberge, M. *Biotechnol. J.* **2006**, *1*, 282−288.
(24) Takikawa, O.; Kuroiwa, T.; Yamazaki, F.; Kido, R. *J. Biol. Chem.* **1988**, *263*, 2041−2048.
(25) Alegre, E.; Lopez, A. S.; Gonzalez, A. *Anal. Biochem.* **2005**, *339*, 188−189.